HHS Public Access

Author manuscript

Analyst. Author manuscript; available in PMC 2017 November 28.

Published in final edited form as:

Analyst. 2016 November 28; 141(24): 6521–6532. doi:10.1039/c6an01448h.

Characterization of Activated Cyclic Olefin Copolymer: Effects of Ethylene/Norbornene Content on the Physiochemical Properties

Colleen E. O'Neil[1], **Scott Taylor**[1], **Kumuditha Ratnayake**[2], **Swathi Pullagurla**[3,6], **Varshni Singh**[2], and **Steven A. Soper**[3,4,5,6]

[1]Department of Chemistry, the University of North Carolina at Chapel Hill, NC, USA

[2]Department of Biomedical Engineering UNC Chapel Hill, NC, USA

[3]Department of Chemistry, the University of Kansas, Lawrence, KS, USA

[4]Department of Mechanical Engineering, the University of Kansas, Lawrence, KS, USA

[5]Ulsan National Institute of Science and Technology, Ulsan, Republic of Korea

[6]Center for Biomodular Multiscale Systems for Precision Medicine

Abstract

The ethylene/norbornene content within cyclic olefin copolymer (COC) is well known to affect the chemical and physical properties of the copolymer, such as the glass transition temperature (T_g) and transparency. However, no work has been reported evaluating the effects of the ethylene/norbornene content on the surface properties of COC following UV/O_3 or O_2 plasma activation. Activation with either O_2 plasma or UV/O_3 is often used to assist in thermal assembly of fluidic devices, increasing the wettability of the surfaces, or generating functional scaffolds for the attachment of biological elements. Thus, we investigated differences in the physiochemical surface properties of various ethylene/norbornene compositions of COC following activation using analytical techniques such as water contact angle (WCA), ATR-FTIR, XPS, TOF-SIMS, UV-VIS, AFM and a colorimetric assay utilizing Toluidine Blue O (TBO). Results showed that increased norbornene content led to the generation of more oxygen containing functionalities such as alcohols, ketones, aldehydes and carboxyl groups when activated with either UV/O_3 or O_2 plasma. Specifically, COC with ~60% norbornene content showed a significantly higher –COOH functional group density when compared to COC with a 50% norbornene content and COC with a 35% norbornene content following UV/O_3 or O_2 plasma activation. Furthermore, COC with large norbornene contents showed a smaller average RMS roughness (0.65 nm) when compared to COC containing low norbornene contents (0.95 nm) following activation making this substrate especially suited for nanofluidic applications, which require smooth surfaces to minimize effects arising from dielectrophoretic trapping or non-specific adsorption. Although all COC substrates showed >90% transparency at wavelengths >475 nm, COC possessing high norbornene contents showed significantly less transparency at wavelengths below 475 nm following activation, making optical detection in this region difficult. Our data showed distinct physiochemical differences in activated COC that was dependent upon the ethylene/norbornene content of the thermoplastic and thus, careful selection of the particular COC grade must be considered for micro- and nanofluidics.

Introduction

The use of polymer substrates for microfluidic applications has been extensively reported in the literature.[1–8] In addition, nanofluidics using polymers is a growing area of research due to the unique analytical capabilities offered by nanofluidic channels that are not accessible using microfluidics.[9–13] Some of the applications for both microfluidics and nanofluidics include microarrays,[14, 15] solid-phase enzymatic reactors,[16–18] solid-phase extractors for nucleic acids and proteins,[19] affinity selection of biological cells,[2, 20, 21] chromatography,[22] and microchip electrophoresis.[23, 24] In all of the aforementioned applications, surface modification of the polymer substrate was required to enable the intended application.

The attractive nature of polymers for micro- and nanofluidic applications include the ability to use a variety of different fabrication strategies that are conducive to mass production, the low-cost of the substrate material and also, the wide selection of different substrate materials that can be employed to suite the particular application.[9, 10, 25] There are two general categories of polymeric materials that have been used in fluidic applications: (1) Elastomers; and (2) thermoplastics. Elastomers, such as polydimethylsiloxane (PDMS), are amorphous polymers with a low to moderate number of cross-links between polymer chains. While the low Young's modulus ensures large deformation upon application of an external load, covalent cross-links help elastomers return to their original shape upon release of the load. Thermoplastics, such as poly(methyl methacrylate), PMMA, polycarbonate, PC, and cyclic olefin copolymer, COC, are linear or branched polymers with higher molecular weights and higher Young's moduli compared to PDMS.[10]

Polymers display a wide range of physiochemical properties allowing for the selection of the optimal material to match the needs of a particular application. A summary of the physiochemical characteristics of common polymers can be seen in Table 1. The wide range of properties, such as glass transition temperature (T_g) and coefficient of thermal expansion (CTE), allow for a diverse range of fabrication techniques, such as injection molding and hot embossing, to make the necessary structures in the device.[10] Furthermore, the range of chemical properties, such as refractive index and optical transmissivity, allow for the use of polymers for unique micro- and nanofluidic applications.

Polymers offer the advantage of being amenable to low-cost fabrication modalities leading to the realization of disposable devices appropriate for *in vitro* diagnostics. PDMS has become a popular material for microfluidics due to its high O_2 and CO_2 permeability and optical transparency (UV to NIR), but it is easily deformable due to its low Young's modulus that can produce low compliance (*i.e.*, inability to maintain its form factor), has unstable surface chemistry and is susceptible to swelling in many solvents.[26, 27] Thermoplastics on the other hand, possess a higher Young's modulus producing better compliance, are conducive to high scale production using replication-based technologies, and their surface chemistry is more stable and can be easily modified using plasmas or UV/O_3 treatments.[9, 10]

COC has become a common thermoplastic used for many microfluidic applications due to its favorable physical characteristics. COC is highly resistant to organic solvents including

polar solvents.[28] This thermoplastic shows low moisture absorption (<0.01%)[28] resulting in high fidelity structures that do not swell. COC also shows excellent optical clarity in the visible and ultraviolet regions of the electromagnetic spectrum.[28] Furthermore, COC has a large range of T_g, low shrinkage and low birefringence.[28, 29]

COC is manufactured commercially by several companies under various trade names and may be referred to as COC or COP (Cyclic Olefin Polymer). The key distinction is the use of either one monomer (COP) or multiple monomers (COC) to generate the thermoplastic. COC can be produced by chain copolymerization of cyclic monomers with ethylene. The cyclic monomer 8,9,10-triborborn-2-ene (norbornene) is used in TOPAS products while 1,2,3,4,4a,5,8,8a-octahydro-1,4:5,8-dimethanonaphthalene (tetracyclododecane) is used by APEL. Manufacturing techniques for COP include ring opening metathesis polymerization of various cyclic monomers followed by hydrogenation (ARTON, Zeonex and Zeonor).[30] Different types of COC can be produced based upon the composition of the monomer units used in its formulation, all which can affect the copolymer's physiochemical properties (see Table 2).

Although COC and other thermoplastics show many favorable properties for fluidic applications, they can be hydrophobic resulting in high surface tension and back pressure, thus making the use of hydrodynamic pumping difficult in micro- and nanofluidic applications. In addition, their surfaces lack functional groups to allow for the covalent attachment of certain biologics to support the intended application. Therefore, activation of the thermoplastic to decrease its hydrophobicity as well as introduce functional groups for surface attachment or modification are necessary. Studies regarding the hydrophobicity of COC have been explored.[2, 31–33] These studies demonstrated that various activation methods (O_2, N_2, Ar plasmas or UV/O_3) can decrease the hydrophobicity of the surface. The UV/O_3 activation process uses a Hg lamp, which continually generates and destroys O_3 yielding a steady-state concentration of strongly oxidizing atomic O. The Hg lamp generates both 185 nm and 254 nm wavelength light. The 185 nm component splits O_2 resulting in O atoms that can react with O_2 to form O_3 while the 254 nm component breaks O_3 into atomic oxygen and O_2, thus yielding a steady-state concentration of atomic O. At sufficiently high energy, UV exposure and oxidative stress can generate radicals within the thermoplastic, which may break or scission polymer chains into smaller fragments, crosslink polymer chains, cause intramolecular rearrangements, and/or react with water or oxidative species to form carboxyl or other O-containing species.[2]

Plasma activation results in a source of highly energetic and reactive species that can interact with the thermoplastic surface. The electrons, ions, and free radicals generated during high energy irradiation of the plasma can promote breakage of C–H and C–C bonds. This leads to shorter polymer chains, the formation of other molecules through recombination reactions and crosslinking. When oxygen is present, chemical interactions between the oxygen molecules and the radicals in the reactive gas create more active radicals, which rapidly initiate chain reactions and form oxygenated products. These products, which may consist of hydroperoxides, carbonyls, carboxylic acids and/or peracids, are polar in nature and contribute to the hydrophilic nature of activated COC.[34]

Jackson *et al.* explored UV/O_3 activation of both COC 6013 from TOPAS and PMMA for the introduction of functional scaffolds to allow for the covalent attachment of antibodies for circulating tumor cell isolation.[2] This study showed that the high UV (254 nm) optical clarity of COC 6013 allowed for deeper penetration of the UV light into high aspect ratio microfluidic channels, compared to PMMA, generating a higher surface load of functional groups, such as carboxyl groups.[2] Hwang *et al.* explored the surface activation of COC purchased from APEX by O_2 plasma treatment and showed that the COC surface acquired oxygen containing polar functional groups such as C-O and C=O, which increased as the plasma treatment time increased with a change in the water contact angle. The change in surface functional groups was accompanied by a slight increase in surface roughness.[31] Roy *et al.* compared N_2 plasma to Ar and O_2 plasma for the activation of COC 6015 from TOPAS by evaluating the adhesion properties, electroosmotic flow (EOF) and the antifouling property of the activated surface. Their results showed a greater decrease in the water contact angle for N_2 plasma compared to Ar and O_2 plasma-activated COC. They attributed this to the introduction of amide groups to the surface, which has a higher polarity than the oxygen containing species generated by Ar or O_2 plasmas.[32]

Despite these studies into the surface activation of COC, no study has explored the differences in activation based on different ethylene/norbornene monomer ratios that can be used in the production of this thermoplastic (see Table 2). One advantage of COC is the range of physical properties that can be achieved based on the difference in the monomer ratios used in its formulation. For example, it is known that an increase in the T_g of COC is correlated with an increase in the mole fraction of norbornene as given by the following equation (Table 2):[28]

$$Norbornene mol\ \% = \frac{(T_g\,(Celcius) + 65)}{4} \quad (1)$$

In copolymers with ≤40% norbornene, the chemical structure of COC is comprised of alternating sequences of norbornene and ethylene units.[30] Higher norbornene contents stiffen the main chain, thus increasing the T_g, tensile strength and decreasing the ductility. Shin *et al.* explored the dependence of T_g on the cyclic monomer content and chemical structure of COC.[30] They reported a linear relationship between the cyclic monomer content and T_g. A difference was observed for COCs with different cyclic monomer units (norbornene or tetracyclododecanediyl). The polycyclic unit, tetracyclododecanediyl, which has a bulkier structure than the bicyclic unit norbornanediyl, leads to a restricted local motion of chain segments and thus higher T_g.

A relationship between norbornene mol% and the refractive index of the substrate has been noted.[35, 36] These investigations showed that an increase in the mol% of norbornene increased the refractive index of the thermoplastic. Liu *et al.* also showed that the copolymer composition distribution had a significant effect on the refractive index and transparency. For the same mol% of norbornene, the transparency of uniform compositions was higher when compared to non-uniform COC.[36]

A clear relationship between the physiochemical properties of COC and its composition has been established; however, the effect of COC composition on the surface properties following activation, either by UV/O_3 or O_2 plasma, has not been explored. This study sought to evaluate the differences in surface characteristics after activation of varying compositions of COC when exposed to UV/O_3 or O_2 plasma with a comparison made to polyethylene (PE), which does not contain the cyclic monomer, norbornene. Water contact angle (WCA), ATR-FTIR, UV/VIS, Toluidine blue O (TBO) assays, XPS, AFM and TOF-SIMS analyses were performed to thoroughly assess the surface chemical properties of three different monomeric ratios of COC from TOPAS. COC from TOPAS is manufactured by a chain copolymerization reaction of norbornene and ethylene. This study investigated COC of the same backbone composition, but different ethylene/norbornene ratios (see Table 2). COC 8007 (35% norbornene) is described as a clear grade with a T_g of 75°C. COC 8007 has a lower elastic modulus and higher elongation than other TOPAS COC grades.[28] COC 6013 (50% norbornene) is described as a clear grade with a T_g of 130°C and COC 6017 (60% norbornene) is a clear grade with a T_g of 170°C.[28] This investigation reports the effects of the norbornene content on the chemical properties of activated COC, which could have profound implications on the performance of micro/nanofluidic devices made from different COC compositions.

Experimental

Reagents and materials

Cyclic olefin copolymers (COC 8007, 6013 and 6017) were purchased from TOPAS Advanced Polymers (Florence KY) in either 1.5 mm or 100 μm thick sheets. Polyethylene, PE, was purchased from Goodfellow (Coraopolis, PA). Frame-sealed incubation chambers were purchased from Bio-Rad (Hercules, CA). Chemicals and reagents used in these studies included sodium carbonate and bicarbonate (Fisher Scientific, Houston, TX); acetic acid (Sigma-Aldrich, St. Louis, MO), and toluidine blue O (TBO; Carolina Biological Supply, Burlington, NC).

Activation of COC

UV/O_3 and O_2 plasma activation was conducted on each substrate. UV/O_3 exposure was performed in a home-built UV activation chamber equipped with a quartz, low-pressure Hg lamp at various intensities (21.85 mW/cm^2, 19.43 mW/cm^2 and 16.01 85 mW/cm^2) for 0, 5, 10 and 15 min. The power of the home-built unit was tested before activation and at the conclusion of the experiments to ensure that the reported powers were accurate. Details showing the power and doses used can be found in Table S1. Oxygen plasma activation was performed in a FEMTO plasma cleaner from Electronic Diener (Ebhausen, Germany) with a gas flow of 10 sccm at various wattages (30 W, 50 W and 70 W) for 0, 12, 36 and 60 s.

Water contact angle (WCA) measurements

WCAs were obtained using a VCA Optima instrument (AST Products). For each of these measurements, 2.0 μL of nanopure water (pH 7.5) was deposited onto the surface followed by collecting the image and measuring the WCA using the manufacturer's software. The

measurements reported were the average of six replicates at various positions on the substrate.

Attenuated total reflectance Fourier transform infrared spectroscopy (ATR-FTIR)

ATR-FTIR measurements were performed on UV/O_3-treated 100 μm thick COC plates. The measurements were not performed on O_2 plasma-treated substrates because the plasma activation only modified the first few monolayers and thus, did not provide sufficient signal for viable observations. ATR-FTIR spectra were acquired from 375–4000 cm^{-1} using an ALPHA FTIR spectrometer and a platinum ATR module (Bruker Optics). Five replicates were performed and spectra were analyzed using Essential FTIR analysis software. Peaks were baseline corrected and total peak area of relevant peaks were assessed.

X-ray photoelectron spectroscopy (XPS)

For XPS measurements, C 1s and O 1s photoelectron signals were acquired using an Axis Ultra DLD X-ray photoelectron spectrometer (Kratos Analytical) under ultra-high vacuum conditions (base pressure 6×10^{-9} Torr) with a monochromatic Al Kα X-ray source, 20 eV pass energy, and 0° electron take-off angle. A charge neutralizer was used to prevent charging. Given an inelastic mean free path of 3–4 nm, ~95% of the resultant signal originated 9–12 nm from the surface.[37–39]

Time of Flight secondary ion mass spectrometry (TOF-SIMS)

TOF-SIMS analyses were conducted using a TOF SIMS V (ION TOF, Inc. Chestnut Ridge, NY) instrument equipped with a Binm+ (n = 1 – 5, m = 1, 2) liquid metal ion gun, Cs+ sputtering gun and electron flood gun for charge compensation. Both the Bi and Cs ion columns were oriented at 45° with respect to the sample surface normal. The instrument vacuum system consisted of a load lock for rapid sample loading and an analysis chamber separated by a gate valve. The analysis chamber pressure was maintained below 5.0×10^{-9} mbar to avoid contamination of the surfaces being analyzed. For the depth profiles acquired in this study, 10 keV low energy Cs+ with 20 nA current was used to create a 120 μm by 120 μm area, and the middle 50 μm by 50 μm area was analyzed using a 0.3 pA Bi3+ primary ion beam. The negative secondary ion mass spectra were calibrated using H-, C-, O-, C3-, C5- and C7-.

UV/VIS

The transparency for non-activated (native) and treated (activated) 100 μm thick COC plates was measured using an Ultrospec 4000 UV/VIS spectrophotometer (Pharmacia Biotech) and acquired between 200 and 800 nm.

Atomic Force microscopy (AFM)

The topographies of non-activated and O_2 plasma treated COC with 3 different norbornene contents were investigated. AFM measurements were performed on the same sample before and after O_2 plasma treatment using the Asylum Research MFP-3D Atomic Force Microscope (tip radius ~2 nm) in repulsive tapping mode at a rate of 1.0 Hz. The Tap300A1-G cantilever tips (Ted Pella) had a frequency of 300 kHz and force constant of 40 N/m. The

scans were taken over a 2 × 2 μm area, which were presented in 3D and RMS surface roughness computed using the manufacturer's software.

Toluidine Blue O (TBO) assay

An in situ incubation chamber (BioRad) was attached to the substrate's surface and filled with 0.1% (w/v) TBO in carbonate buffer (50 mM, pH = 10.5). After 15 min, the substrate was submersed in the same buffer for 15 min and air dried. TBO was desorbed using 40% acetic acid (d = 1.0196 g mL^{-1}), collected in a pre-weighed microfuge tube, and analyzed with an Ultrospec 4000 UV/Vis spectrophotometer (Pharmacia Biotech) against a 40% acetic acid blank.

Results and Discussion

Activation of thermoplastic surfaces by UV/O_3 or O_2 plasma results in photo-oxidation and chain scissioning of the thermoplastic.[40] Photo-oxidation results in the formation of radicals and chain scissioning leads to the presence of shorter polymer chains compared to the non-treated thermoplastic.[2, 40] Prolonged exposure can result in photoablation of the surface as well.[2, 40] Activation with oxygen sources typically results in the formation of oxygen containing groups on the surface such as alcohols, aldehydes, ketones and carboxyl groups. Previous work explored the density and distribution of these generated functional groups showing that COC 6013 had greater –COOH surface functional group densities compared to PMMA with a heterogeneous distribution of these groups following activation.[2, 41] But, no work has explored differences in the generation of these functional groups between different monomer compositions of COC.

Although most fluidic applications require the activation of the thermoplastic to generate a substrate with higher surface energy, there are different requirements for the degree of activation. For instance, the immobilization of biologics, such as antibodies, onto the surface requires the generation of a high number of surface functional groups.[2] However, electrophoresis applications may require a reduced surface charge for the generation of a smaller electroosmotic flow (EOF). Application specific requirements of thermoplastic devices requires a thorough understanding of the effect of substrate composition on the extent of activation. This understanding will allow for the informed and precise selection of a thermoplastic for a specific fluidic application. Thus, we embarked upon looking at different types of COC in terms of the physiochemical properties following UV/O_3 or O_2 plasma activation. In this study, TOPAS COC was investigated for several reasons. First, TOPAS has the largest range of T_g COCs that are commercially available, which results from the large range of norbornene contents in the copolymer (see equation 1). Because we were interested in understanding the effects of the ethylene/norbornene content on the physiochemical properties of COC following activation, the large range of monomer contents associated with the TOPAS COC permitted these evaluations. Second, the process of manufacturing COC varies between vendors (see Introduction). Because we sought to understand the difference in physiochemical properties based on the ethylene/norbornene content of the material only, we did not want differences in formulations to confound the results. Lastly, the cyclic molecule used by different vendors varies. Because only the

norbornene content in the copolymer was the focus of this investigation, different COC sources would add another variable to the study.

WCAs of native and activated COC and PE

For the sessile WCA measurements performed herein, nanopure (pH 7.5) water was deposited (2 μL) onto the surface of native and activated substrates and the WCA was determined to evaluate the surface hydrophilicity/hydrophobicity, which is indicative of the degree of formation of polar functional groups on the surface generated by the activation process. UV/O_3 and O_2 plasma-activated COC and PE results are shown in Figure 1. All native COC and PE surfaces showed high WCAs indicative of a more hydrophobic surface. Upon activation with UV/O_3 (Figure 1 a–c), the WCA decreased indicating a more hydrophilic surface likely due to the generation of polar surface groups as a result of activation. For PE following activation, the minimum WCA was significantly higher, ~60°, compared to all of the COC grades. At 21.85 mW/cm^2 UV/O_3 exposure for 15 min, we did see an increase in the contact angle for PE (Figure 1c), which could have arisen from surface ablation or further radical reactions roughening the surface.[31] COC 8007, which has ~35% norbornene content, showed a minimum WCA of 41° for 16.01 mW/cm^2 after 10 min of irradiation, 38° for 19.43 mW/cm^2 after 15 min and 37° for 21.85 mW/cm^2 after 5 min. The specific dose of each treatment regimen can be found in Table S1. COC 6013, which has a ~50% norbornene content, showed a minimum contact angle of 34° for 16.01 mW/cm^2 after 10 min, 31° for 19.43 mW/cm^2 after 5 min and 37° for 21.85 mW/cm^2 after 5 min. COC 6017, which has ~60% norbornene content, showed a minimum WCA of 32° for 16.01 mW/cm^2 after 10 min, 29° for 19.43 mW/cm^2 after 5 min and 29° for 21.85 mW/cm^2 after 15 min. We also noticed an increase in the WCA for longer exposure times after the minimum had been reached, most likely due to surface roughening. Overall, COC 8007 showed a significantly higher WCA (more hydrophobic) when compared to COC 6013 and COC 6017.

O_2 plasma-activated COC and PE results can be seen in Figure 1 d–f. Similar trends were observed when compared to the UV/O_3-activated surfaces. A sharp decrease in the WCA occurred after the first 10 s of exposure to O_2 plasma regardless of the dose. In contrast to UV/O_3 activation, we did not see an increase in the WCA after prolonged exposure. PE had the highest WCA of the substrates investigated with a value of 57°, which was similar to the WCA obtained through UV/O_3 exposure. COC 8007 maintained an average WCA of 41° regardless of the activation dose, which was significantly higher than COC 6013, which had an average WCA of 33°. COC 6017 had an average WCA minimum of 31°.

The WCA data indicated that there was a difference in the hydrophilicity of the surface after activation, which was dependent on the norbornene content of the thermoplastic. We note that an increase in surface roughness may also contribute to a higher WCAs for activated thermoplastics. Thus, AFM measurements were carried out to deduce potential roughening effects (see below). Two different processes could occur during activation irrespective of the activation source; Photo-oxidation and chain scissioning reactions. The presence of low molecular weight fragments on the surface may affect the WCA measurement. For example, thermoplastics such as PMMA, have shown a drop in the WCA following activation

followed by a higher WCA after being rinsed with a solvent, which removes the low molecular weight fragments.[2] However, literature has shown that the generation of these low molecular weight fragments occurs to a lesser degree in COC compared to PMMA.[2]

ATR-FTIR analysis of UV/O_3-activated COC and PE

To understand the chemical functional groups responsible for the decrease in the WCA of activated COCs and PE, ATR-FTIR experiments were performed. As stated, ATR-FTIR has penetration depths ranging from 0.5–2 μm into the bulk material;[42] UV/O_3-activated surfaces showed sufficient ATR-FTIR signals as the activation process occurs into the bulk of the thermoplastic, whereas O_2 plasma activation occurs only within the first few monolayers. ATR-FTIR spectra for all COC types and PE exposed to 21.85 mW/cm^2 UV/O_3 for 15 min can be seen in Figure 2a. All samples showed peaks ranging from 2940–2860 cm^{-1}, which corresponded to the -CH stretching mode (ethylenic H and aldehydic H) and a peak at 1454 cm^{-1}, which corresponded to the -CH bending mode; these are in good agreement with previously reported results.[34, 43, 44] We observed a decrease in the overall peak intensity and peak area in this spectral region for activated substrates compared to the native material. We did observe an increased peak intensity around 1744 cm^{-1} for all activated substrates with those thermoplastics containing greater norbornene contents showing the greatest change. This region is associated with the presence of carbonyl groups that could have been produced from photo-oxidation reactions occurring during activation and can be seen in Figure 2b.[32, 44] The greatest carbonyl intensity was correlated with the lowest alkane intensity after activation. Furthermore, an ATR-FTIR peak in the 3500–3600 cm^{-1} range was present for the activated substrates. This peak indicated the presence of hydroxyl groups (–OH), which could also contribute to the increased hydrophilic nature of the COC surface following activation and was shown to have the greatest intensity for COC substrates with the highest norbornene content. The native COC and PE substrates did not show absorbance in the carbonyl or hydroxyl regions within the IR spectrum, further supporting that activation results in the generation of oxygen containing functional groups.

To quantify the difference in oxygen containing functional groups between the various thermoplastics, the oxygen to carbon ratio for each thermoplastic was plotted as a function of the exposure time as seen in Figure 2 c–f. For all substrates, greater O/C ratios were seen for 21.85 mW/cm^2 when compared to 19.43 mW/cm^2 and 16.01 mW/cm^2 for similar exposure times, which is to be expected due to the higher dose. PE showed little change in the O/C ratio with increased dose, with a maximum O/C ratio of 0.03. The maximum O/C ratios were 0.24 for COC 8007 (lowest norbornene content), 0.60 for COC 6013 and 0.75 for COC 6017 (highest norbornene content). The greatest O/C ratio was observed for the thermoplastic with the greatest norbornene content, which agreed with the increasing hydrophilicity of thermoplastics with greater norbornene mol% observed with the WCA data. In addition, the increase in the O/C ratio from the native substrate to substrates exposed to 5 min of 21.85 mW/cm^2 UV/O_3 treatment showed a linear relationship (R^2 = 0.99) with the norbornene content (Figure S1). After the 5 min exposure, there was still an increase in the O/C ratio, however, the percent increase was not as dramatic for all of the substrates as that seen within the first 5 min of activation. For instance, COC 6017 showed a 22-fold increase in the O/C ratio from 0 min to 5 min exposure to 21.85 mW/cm^2 UV/O_3 activation,

but only a 2-fold increase from 5 min to 10 min exposure. Figure 3 shows the change in the carbonyl peak area for all substrates. Once again, there was a significant difference in the carbonyl peak area for all substrates with COC 6017 showing the greatest peak area and PE showing the least. The peak area increased with the norbornene content as observed in the O/C ratio (Figure 2 c–f).

X-Ray photoelectron spectroscopy (XPS)

We further explored the O/C carbon ratio using XPS, which interrogates electrons released from 1–10 nm of the surface and is thus, more surface sensitive compared to ATR-FTIR. Figure 4a shows the high resolution C 1s spectra for COC 8007 and COC 6017 activated with 21.85 mW/cm^2 UV/O_3 for 15 min, while Figure 4b shows the O/C ratio versus exposure time for COC and PE samples activated with 21.85 mW/cm^2 UV/O_3 radiation. In the full XPS spectra, we saw almost no oxygen containing functional groups before activation of the thermoplastics, but we did observe a large increase in the oxygen content after activation (Figure S2). All samples showed a dramatic increase in the O/C ratio after 5 min exposure with COC 6017 showing a significantly higher O/C ratio when compared to all other samples with a 100-fold increase in the O/C ratio after 5 min exposure. This trend continued with further exposure to UV/O_3 radiation with COC 6017 showing significantly higher O/C ratios for all exposure times as supported by the high resolution C 1s spectra (Figure 4a). The highest O/C ratio achieved for each thermoplastic was 31.6%, 23.7%, 18% and 13% for COC 6017, 6013, 8007 and PE, respectively. The highest O/C ratio was observed after 15 min exposure for all thermoplastics except COC 8007 (lowest norbornene content), which showed the greatest O/C ratio after 10 min. This may be due to the greater percentage of ethylene chains within the thermoplastic, which may undergo chain scissioning reactions and further radical reactions potentially removing any generated oxygen containing functional groups.[2] Taken together, both ATR-FTIR and XPS showed significantly higher oxygen containing functional groups for COC containing greater norbornene contents.

UV-VIS spectroscopy of COC and PE

One attractive property of COC is its excellent optical properties in its non-activated form, making it appropriate for microfluidic or nanofluidic applications requiring optical detection. Activation of the thermoplastic, however, may have an effect on the optical transparency. Our investigations here were aimed to determine how the norbornene content affected the optical clarity of the material following UV/O_3 or O_2 plasma activation. For these measurements, 100 μm thick plates were activated via O_2 plasma (70 W for 60 s) and UV/O_3 (21.85 mW/cm^2 for 15 min) and the percent transmittance was determined using UV/VIS spectrophotometry. Percent transmittance is dependent on the thickness of the substrate as observed by Khanarian *et al.*[29] and therefore, we selected a 100 μm thick plate in all cases, which is a thickness typically used as a cover plate for microfluidic devices.[12, 45–47]

Figure 5a shows the percent transmittance as a function of wavelength for O_2 plasma treated COC, while Figure 5b shows the percent transmittance as a function of wavelength for UV/O_3-activated COC. Overall, O_2 plasma-activated substrates showed no deviation from

the native spectra, with 90% transmittance (T) at wavelengths >400 nm while UV/O_3-activated substrates had significant decreases in their %T when compared to the native substrates (Figure S3). As stated, these values were not significantly different for O_2 plasma treated substrates. All substrates showed a decrease in transmissivity at 254 nm after UV/O_3 exposure with COC 6017 showing the greatest decrease (38.7% decrease) and COC 8007 showing the smallest (16.8 %) decrease. Our data indicated that greater surface activation was present with higher norbornene contents, which may be the cause for decreased UV transmissivity. Beyond 475 nm, all substrates regardless of composition or activation showed approximately 90% transmissivity.

TOF-SIMS

It has been speculated that UV/O_3 activation penetrates within the bulk of the substrate due to the UV transparency of COC (see Figure S3 and Figure 5b), but to our knowledge no published data has supported this claim. We sought to investigate the activation depth of COC with UV/O_3 treatment as well as differences between various COC compositions. TOF-SIMS can secure elemental and molecular information with high spatial and mass resolution.[48] With dual beam operation, depth profile of ions can be obtained. The Cs+ ion gun ablated the surface (~1 nm/s) while the Bi^{3+} ion gun was used to generate secondary ions for analysis. For these experiments, we compared COC 8007 and COC 6017 both activated with 21.85 mW/cm^2 UV/O_3 for 15 min to the native thermoplastic.

As can be seen in Figure 6, UV/O_3-activated COC 8007 and COC 6017 showed a significant increase in the O^- content of the substrate compared to the non-activated substrate. The greater degree of oxygen containing functional groups for COC 6017 when compared to COC 8007 was in agreement with both the XPS and ATR-FTIR data. Consistent with our supposition that UV/O_3 activation also produced modifications into the bulk (see the ATR-FTIR section), the presence of oxygen-containing species were found at depths up to 450 nm, albeit with a decreased amount compared to the surface. TOF-SIMS profiles of O_2 plasma-activated COC 8007 and COC 6017 substrates were investigated as well, but the O^- ion only showed a significant difference from the native COC for the first seconds of sputtering (data not shown) indicating that O_2 plasma activation was restricted to the surface.

It is interesting to note that although native COC 6017 showed 30% less transparency than native COC 8007 at 254 nm, it showed greater O content deeper within the substrate. We would anticipate to see a greater presence of O species for COC 8007 deeper within the bulk polymer because the UV activating radiation should penetrate deeper into the substrate due to its higher transparency.

Assessment of –COOH surface functional group density on activated COC using the TBO assay

As previously discussed, the generation of specific functional groups on the surface of thermoplastics during activation is key for various fluidic applications. Of great interest is the generation of surface –COOH groups that can serve as a functional scaffold for the attachment of biological entities, such as antibodies,[2] or for deprotonation to generate surface charge that can control the electroosmotic flow.[47] Previous literature has shown

differences in the surface –COOH functional group density and heterogeneity of COC 6013 compared to PMMA.[2, 45] Here, we sought to investigate the differences in various compositions of COC on the surface load of –COOH groups generated via activation. To investigate these differences, we utilized a colorimetric assay with a cationic dye, TBO, which binds electrostatically (1:1) to deprotonated –COOH groups. The TBO assay not only probes surface functional groups, but also can probe molecules in underlying layers due to the generation of a porous surface caused by photo-fragmentation reactions occurring on surfaces. Consequently, absolute carboxyl surface densities were not reported, rather relative densities (see Figure 7). COC 6017 showed higher ($p < 0.001$) –COOH functional group densities compared to COC 6013 and COC 8007. While TBO can penetrate into the bulk of the thermoplastic due to photo-fragmentation, the degree of photo-fragmentation is known to be minimal for COC.[2]

AFM to determine surface roughness following activation

As previously discussed, surface roughness can have an effect on the WCA. Furthermore, surface roughness can be problematic for many fluidic applications, especially for nanofluidics as it can generate undesired wall interactions or dielectrophoretic trapping.[46] Thus, we explored differences in surface roughness of various O_2 plasma-activated COC thermoplastics. Only O_2 plasma activation was explored here because this is commonly used for the assembly of nanofluidic devices, and surface roughness can play a significant role in determining the functional properties of nanofluidic devices.[9, 12, 17, 25, 41, 46, 47] For these studies, the initial RMS surface roughness of native COC thermoplastics was measured using AFM. Then, each substrate was exposed to 30 s of 50 W O_2 plasma, as this treatment can serve as an effective strategy for thermal fusion bonding cover plates to thermoplastic substrates,[46] and the RMS roughness was re-measured following this treatment. The raw data is presented in Table S2. In Figure 8, 3D AFM plots of native COC 8007 (Figure 8a) and native COC 6017 (Figure 8c) as well as O_2 plasma treated COC 8007 (Figure 8b) and COC 6017 (Figure 8d) substrates are shown. As can be seen, O_2 plasma activation increased the surface roughness of both COC 8007 and COC 6017. Figure 8e plots the difference in the O_2 plasma treated and native substrate RMS roughness as a function of the norbornene mol%, which indicated that as the norbornene mol% increased, a decrease in RMS roughness of the activated surface was seen. The process of O_2 plasma activation promotes the breakage of C–H and C–C bonds leading to the generation of shorter polymer fragments and surface ablation, both of which can roughen the activated surface. Our AFM data indicated that increased norbornene mol% may decrease the chain scissioning observed while the spectroscopy data showed greater formation of oxygenated products for thermoplastics with greater norbornene contents.

Conclusions

COC is an attractive thermoplastic for micro- and nanofluidics due to its resistance to organic solvents, low moisture absorption, optical clarity in the visible and ultraviolet regions of the electromagnetic spectrum, a large range of T_g, low shrinkage and low birefringence.[28, 29] These properties allow for a wide range of fabrication modalities that can be employed to generate structures across many different length scales with high

compliance. However, due to its hydrophobic nature, activation of COC is required to increase its surface energy allowing for more favorable wettability. The physiochemical properties of COC are dependent on the composition of COC and our study aimed to investigate the effects of the ethylene/norbornene content of COC on these properties following activation. These physical property changes manifest themselves from alterations in the surface O-content, which can affect microfluidic and nanofluidic operational performance, such as loading of biologics, wettability, EOF and/or electrokinetic separations.

Several analytical approaches were used to probe the surface characteristics of activated COC such as the sessile WCA measurements, ATR-FTIR, XPS, TOF-SIMS, UV-VIS, AFM and a colorimetric assay utilizing TBO. WCA analysis indicated that an increased norbornene content led to a more hydrophilic surface following UV/O_3 or O_2 plasma activation, which was supported by spectrophotometric analysis (ATR-FTIR and XPS); COC 6017 (~60% norbornene) had higher oxygen containing functional groups compared to COC 8007 (~35% norbornene). TBO analyses indicated that COC with high norbornene contents contained higher –COOH group densities relative to COC types with lower norbornene contents, which may be important for fluidic applications requiring large EOFs or functional scaffolds for the attachment of various biologics. Furthermore, TOF-SIMS confirmed that COC 6017 contained O-bearing functional groups 450 nm deep into the thermoplastic when activated by UV/O_3, while O_2 plasma only activated the surface of the thermoplastic. AFM results coupled with our ATR-FTIR data indicated that increased O containing groups of COC with greater norbornene content did not necessarily lead to a rougher surface. In fact, greater norbornene content resulted in a decrease in the RMS roughness making COC with the highest norbornene content an attractive substrate for nanofluidic applications requiring surfaces that are not prone to excessive wall interactions and/or dielectrophoretic trapping. Despite the greater norbornene content, COC did show a decrease in the UV transparency, especially for UV/O_3 treatment.

Our data provides key insights into the selection of a COC type and activation protocol for a particular fluidic application. Taken together, our data suggests that COC with a high norbornene content is advisable when a high load of –COOH functional groups are required, for example when device require the immobilization of biorecognition elements for affinity-based assays, micro- or nanoelectrophoresis requiring a strong and stable EOF or nanofluidic applications requiring a highly wettable surface. COC with a low content of norbornene, despite showing the lowest –COOH load and oxygen containing surface, would be an excellent choice for optical detection <450 nm due to its high transmissivity in this region. Furthermore, Leech *et al.* studied the hot embossing of COC as a function of the norbornene content and found that at temperatures above the T_g, the embossed patterns were independent of the norbornene content.[49] Thus, high fidelity replication is independent of the norbornene content.

Supplementary Material

Refer to Web version on PubMed Central for supplementary material.

Acknowledgments

The authors would like to thank the National Institutes of Health (P41EB020594), the National Science Foundation (1507577), Research Fund (1.130090.01) of Ulsan National Institute of Science and Technology) and Roche for financial support of this work. CEO thanks the National Science Foundation for support through a summer fellowship program (EAPSI). SAS would like to thank Prof. Craig Lunte for his many years of consultation and friendship, which has made a mark on his career.

References

1. Henry AC, Tutt TJ, Galloway M, Davidson YY, McWhorter CS, Soper SA, McCarley RL. Analytical Chemistry. 2000; 72:5331–5337. [PubMed: 11080884]
2. Jackson JM, Witek MA, Hupert ML, Brady C, Pullagurla S, Kamande J, Aufforth RD, Tignanelli CJ, Torphy RJ, Yeh JJ, Soper SA. Lab on a Chip. 2014; 14:106–117. [PubMed: 23900277]
3. Pullagurla SR, Witek MA, Jackson JM, Lindell MAM, Hupert ML, Nesterova IV, Baird AE, Soper SA. Analytical Chemistry. 2014; doi: 10.1021/ac5007766
4. Gulliksen A, Anders Solli L, Stefan Drese K, Sorensen O, Karlsen F, Rogne H, Hovig E, Sirevag R. Lab on a Chip. 2005; 5:416–420. [PubMed: 15791339]
5. Park S, Lee J, Yoon H, Kim B, Sim S, Chae H, Yang S. Biomed Microdevices. 2008; 10:859–868. [PubMed: 18553169]
6. Pu Q, Elazazy MS, Alvarez JC. Analytical Chemistry. 2008; 80:6532–6536. [PubMed: 18666781]
7. Tan HY, Loke WK, Tan YT, Nguyen NT. Lab on a Chip. 2008; 8:885–891. [PubMed: 18497907]
8. Wang YX, Zhou Y, Balgley BM, Cooper JW, Lee CS, DeVoe DL. Electrophoresis. 2005; 26:3631–3640. [PubMed: 16136528]
9. Chantiwas R, Hupert ML, Pullagurla SR, Balamurugan S, Tamarit-Lopez J, Park S, Datta P, Goettert J, Cho YK, Soper SA. Lab on a Chip. 2010; 10:3255–3264. [PubMed: 20938506]
10. Chantiwas R, Park S, Soper SA, Kim BC, Takayama S, Sunkara V, Hwang H, Cho YK. Chemical Society Reviews. 2011; 40:3677–3702. [PubMed: 21442106]
11. Uba FI, Pullagurla SR, Sirasunthorn N, Wu J, Park S, Chantiwas R, Cho YK, Shin H, Soper SA. Analyst. 2015; 140:113–126. [PubMed: 25369728]
12. Weerakoon Ratnayake KM, Uba FI, Oliver-Calixte NJ, Soper SA. Analytical Chemistry. 2016; doi: 10.1021/acs.analchem.5b04065
13. Sivanesan P, Okamoto K, English D, Lee CS, DeVoe DL. Analytical Chemistry. 2005; 77:2252–2258. [PubMed: 15801761]
14. Roy E, Stewart G, Mounier M, Malic L, Peytavi R, Clime L, Madou M, Bossinot M, Bergeron MG, Veres T. Lab on a Chip. 2015; 15:406–416. [PubMed: 25385141]
15. Soper SA, Hashimoto M, Situma C, Murphy MC, McCarley RL, Cheng YW, Barany F. Methods. 2005; 37:103–113. [PubMed: 16199178]
16. Lee J, Soper SA, Murray KK. Rapid Communications in Mass Spectrometry. 2011; 25:693–699. [PubMed: 21337630]
17. Oliver-Calixte NJ, Uba FI, Battle KN, Weerakoon-Ratnayake KM, Soper SA. Analytical Chemistry. 2014; 86:4447–4454. [PubMed: 24628008]
18. Chen G, McCarley RL, Soper SA, Situma C, Bolivar JG. Chemistry of Materials. 2007; 19:3855–3857.
19. Battle KN, Jackson JM, Witek MA, Hupert ML, Hunsucker SA, Armistead PM, Soper SA. Analyst. 2014; 139:1355–1363. [PubMed: 24487280]
20. Torphy RJ, Kamande JW, Tignanelli CJ, Moffit RA, Soper SA, Yeh J. Journal of Surgical Research. 179:340.
21. Dharmasiri U, Njoroge SK, Witek MA, Adebiyi MG, Kamande JW, Hupert ML, Barany F, Soper SA. Analytical Chemistry. 2011; 83:2301–2309. [PubMed: 21319808]
22. Xia H, Murray K, Soper S, Feng J. Biomed Microdevices. 2012; 14:67–81. [PubMed: 21915645]
23. Shadpour H, Musyimi H, Chen J, Soper SA. Journal of Chromatography A. 2006; 1111:238–251. [PubMed: 16569584]

24. Njoroge SK, Witek MA, Battle KN, Immethun VE, Hupert ML, Soper SA. Electrophoresis. 2011; 32:3221–3232. [PubMed: 22038569]
25. Wu J, Chantiwas R, Amirsadeghi A, Soper SA, Park S. Lab on a Chip. 2011; 11:2984–2989. [PubMed: 21779601]
26. McDonald JC, Duffy DC, Anderson JR, Chiu DT, Wu H, Schueller OJA, Whitesides GM. Electrophoresis. 2000; 21:27–40. [PubMed: 10634468]
27. Sia SK, Whitesides GM. Electrophoresis. 2003; 24:3563–3576. [PubMed: 14613181]
28. TOPAS. Cyclic Olefin Copolymer. http://www.topas.com/sites/default/files/files/TOPAS_Brochure_E_2014_06(1).pdf
29. Khanarian G, Celanese H. OPTICE. 2001; 40:1024–1029.
30. Shin, JYP Ju Young, Liu, Chenyang, He, Jiason, Kim, Sung Chul. Pure and Applied Chemistry. 2005; 77:801–814.
31. Hwang S-J, Tseng M-C, Shu J-R, Her Yu H. Surface and Coatings Technology. 2008; 202:3669–3674.
32. Roy S, Yue CY. Plasma Processes and Polymers. 2011; 8:432–443.
33. Tsao CW, Hromada L, Liu J, Kumar P, DeVoe DL. Lab on a Chip. 2007; 7:499–505. [PubMed: 17389967]
34. Roy S, Yue CY, Lam YC, Wang ZY, Hu H. Sensors and Actuators B: Chemical. 2010; 150:537–549.
35. McKnight AL, Waymouth RM. Macromolecules. 1999; 32:2816–2825.
36. Liu S, Yao Z, Chen L, Dai BB, Cao K, Li BG, Zhu S. Journal of Applied Polymer Science. 2011; 121:707–710.
37. Seah MP, Dench WA. Surface and Interface Analysis. 1979; 1:2–11.
38. Mitchell DF, Clark KB, Bardwell JA, Lennard WN, Massoumi GR, Mitchell IV. Surface and Interface Analysis. 1994; 21:44–50.
39. Powell CJ, Jablonski A, Tanuma S, Penn DR. Journal of Electron Spectroscopy and Related Phenomena. 1994; 68:605–616.
40. R, BG., Rabek, JF. Photodegradation, photooxidation, and photostabilization of polymers, principles and applications. Wiley; London, New York: 1975.
41. Oneil CE, Jackson JM, Shim SH, Soper SA. Analytical Chemistry. 2016; 88:3686–3696. [PubMed: 26927303]
42. Mirabella, FM. Internal reflection spectroscopy: theory and applications. Marcel Dekker; New York: 1993.
43. Yang TCK, Lin SSY, Chuang TH. Polymer Degradation and Stability. 2002; 78:525–532.
44. Forsyth J, Pereña JM, Benavente R, Pérez E, Tritto I, Boggioni L, Brintzinger H-H. Macromolecular Chemistry and Physics. 2001; 202:614–620.
45. Oneil CE, Jackson JM, Shim SH, Soper SA. Analytical Chemistry. 2016; doi: 10.1021/acs.analchem.5b04472
46. Uba FI, Hu B, Weerakoon-Ratnayake K, Oliver-Calixte N, Soper SA. Lab on a Chip. 2015; 15:1038–1049. [PubMed: 25511610]
47. Uba FI, Pullagurla S, Sirasunthorn N, Wu J, Park S, Chantiwas R, Cho YK, Shin H, Soper SA. Analyst. 2014; 139
48. Belu AM, Graham DJ, Castner DG. Biomaterials. 2003; 24:3635–3653. [PubMed: 12818535]
49. Leech PW. Journal of Micromechanics and Microengineering. 2009; 19:055008.

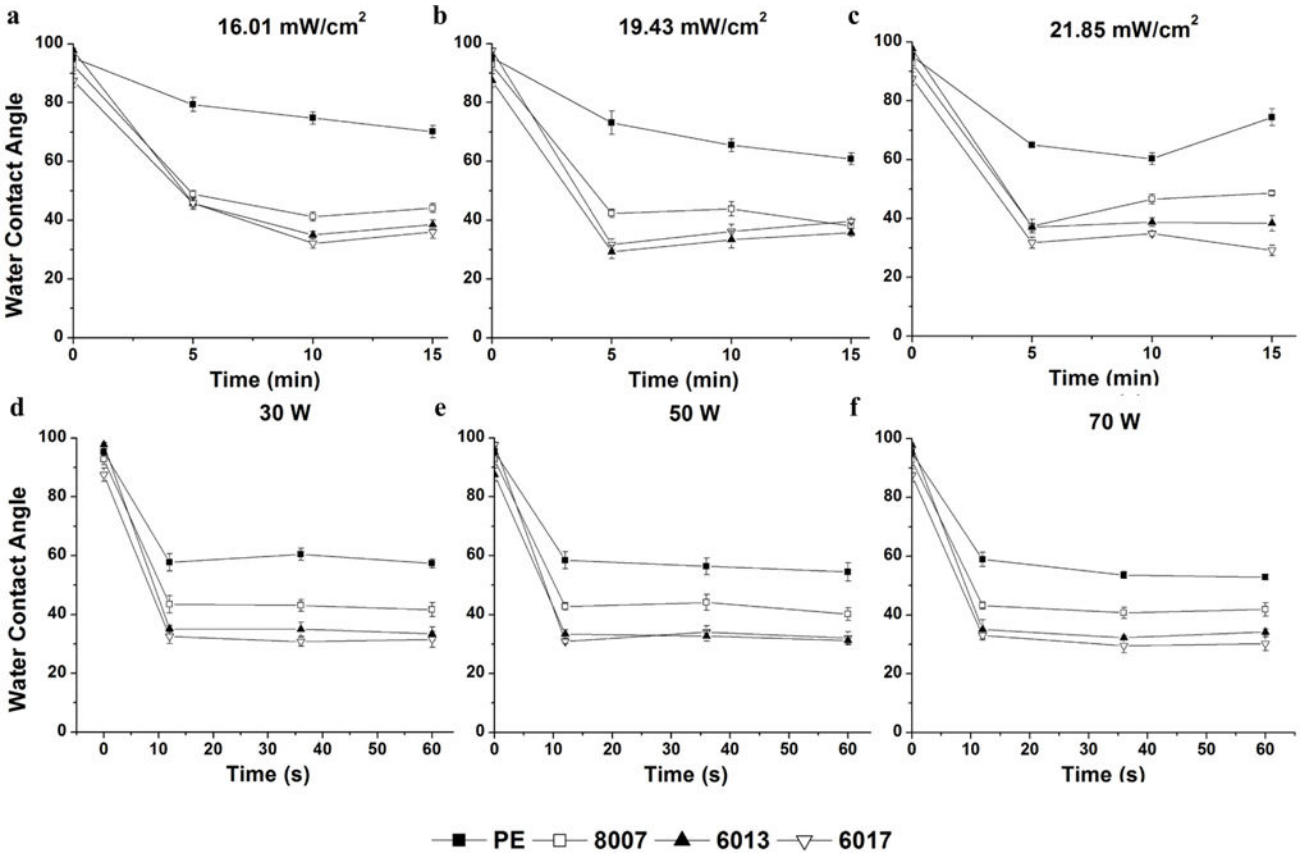

Figure 1.

WCAs for activated TOPAS COC and PE. a) 16.01 mW/cm^2 UV/O_3-activated COC; b) 19.43 mW/cm^2 UV/O_3-activated COC; c) 21.85 mW/cm^2 UV/O_3-activated COC; d) 30 W O_2-activated COC; e) 50 W O_2-activated COC; and f) 70 W O_2-activated COC. Error bars show ±std of average WCA (n=5).

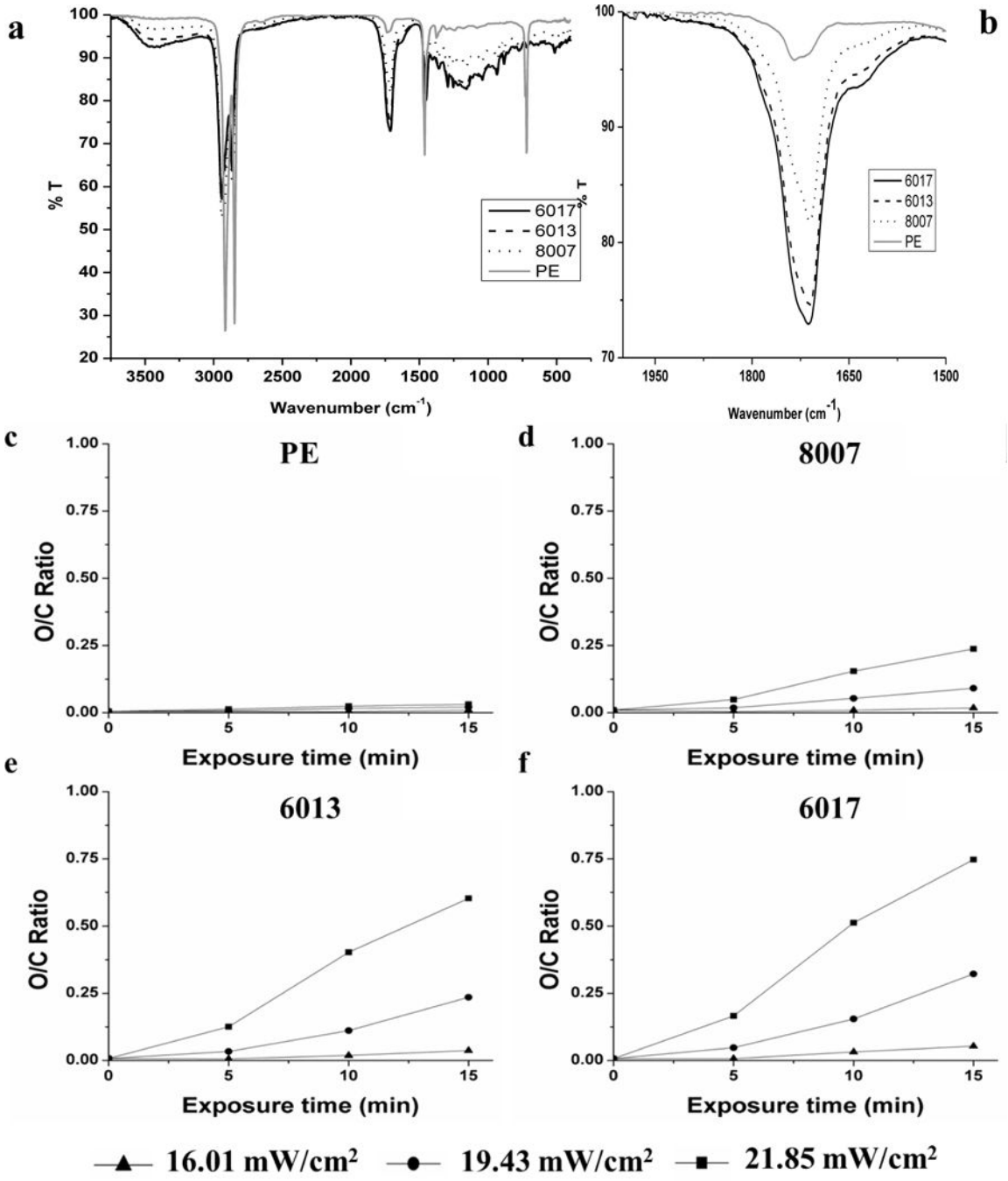

Figure 2.

ATR-FTIR analysis of UV/O_3-activated TOPAS COC and PE. a) ATR-FTIR spectrum of PE and COC exposed to 21.85 mW/cm^2 of UV/O_3 for 15 min. b) Sub-section of the spectrum seen in (a) showing the carbonyl region of the spectrum. c–f) Oxygen to carbon ratio versus exposure time for various power levels of UV/O_3 activation for PE, COC 8007, COC 6013 and COC 6017, respectively. The lines connecting the data points do not represent a functional relationship within a series, but are used for clarity of presentation only.

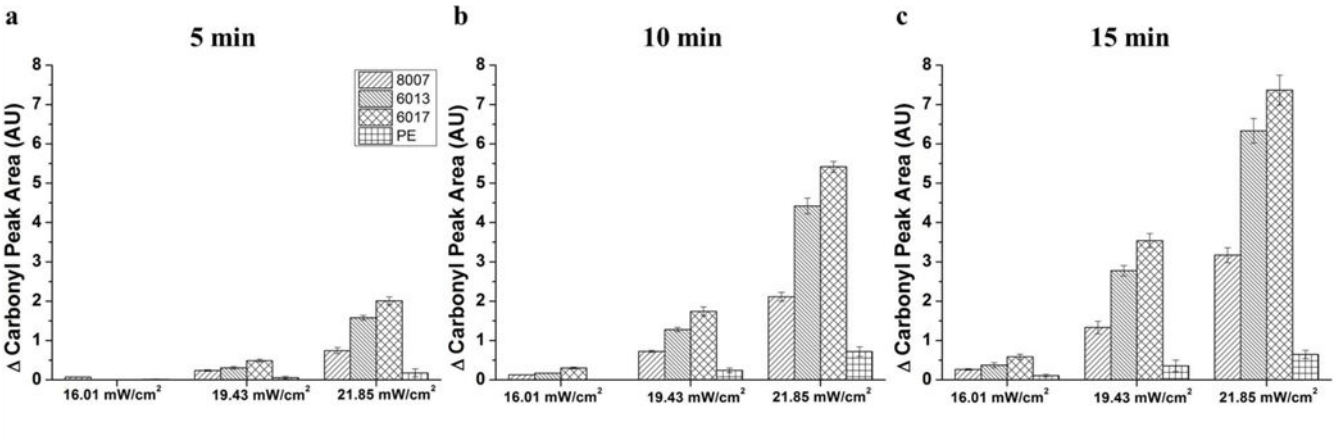

Figure 3.

Change in the carbonyl peak area of the ATR-FTIR spectra versus the UV/O_3 activation power for: a) 5 min exposure; b) 10 min exposure; and c) 15 min exposure. Error bars represent ±std of the average carbonyl peak area (n=5)

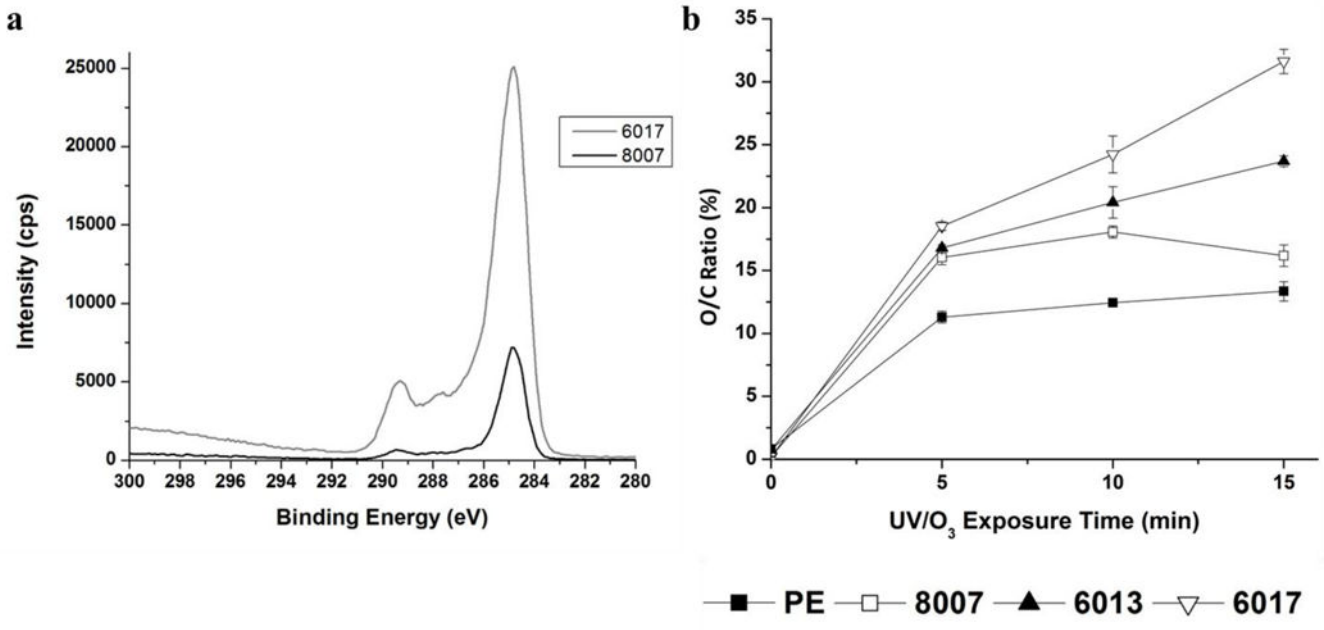

Figure 4.

a) High resolution C 1s XPS spectra for UV/O_3-activated COC 6017 and COC 8007 (21.85 mW/cm^2 for 15 min). b) O/C ratio versus exposure time for 21.85 mW/cm^2 UV/O_3-activated PE (filled square), COC 8007 (open square), COC 6013 (filled triangle) and COC 6017 (open triangle). Error bars represent ±std of the average O/C ratio (n=3).

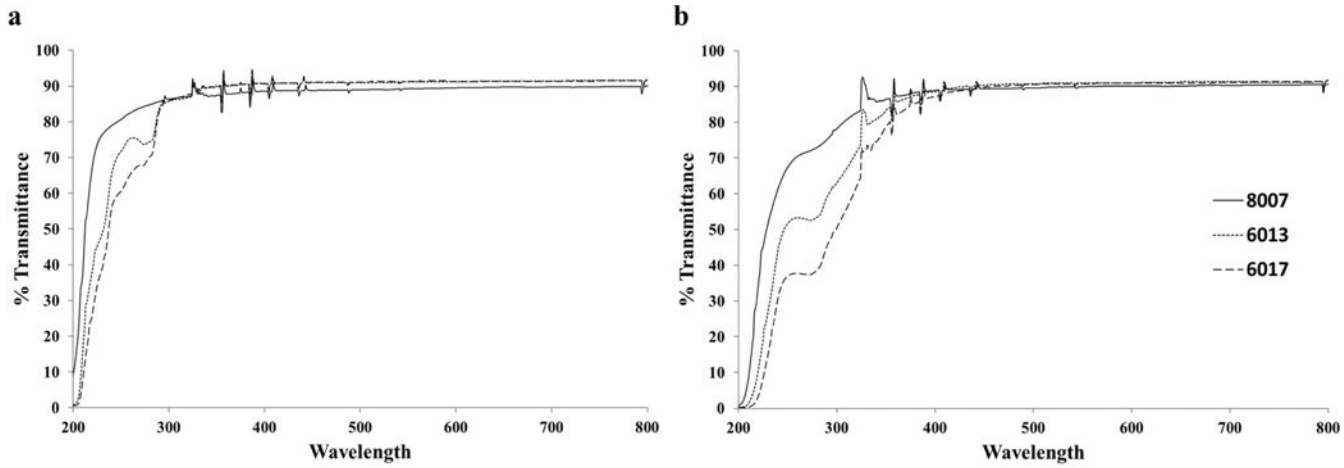

Figure 5.

UV-VIS spectrum for TOPAS COC after a) 70 W O_2 exposure for 60 s and b) 21.85 mW/cm^2 UV/O_3 exposure for 15 min. All spectrum showed a decrease in the transmittance when compared to the native substrates (Figure S3).

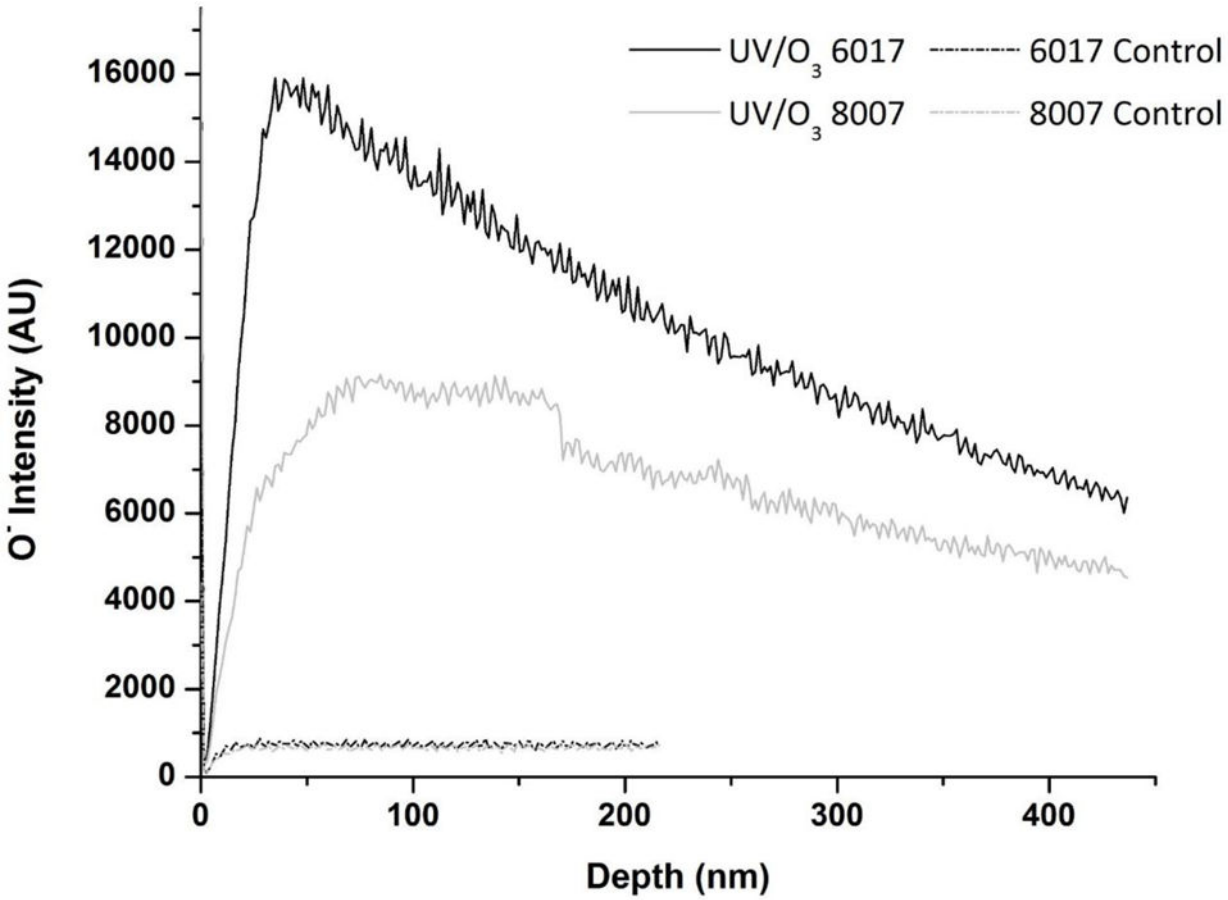

Figure 6.

TOF-SIMS data showing the intensity of the oxygen ion versus depth for 21.85 mW/cm^2 UV/O_3-activated COC 6017 (black) and COC 8007 (gray) compared to native COC 6017 (black dash) and native COC 8007 (gray dash).

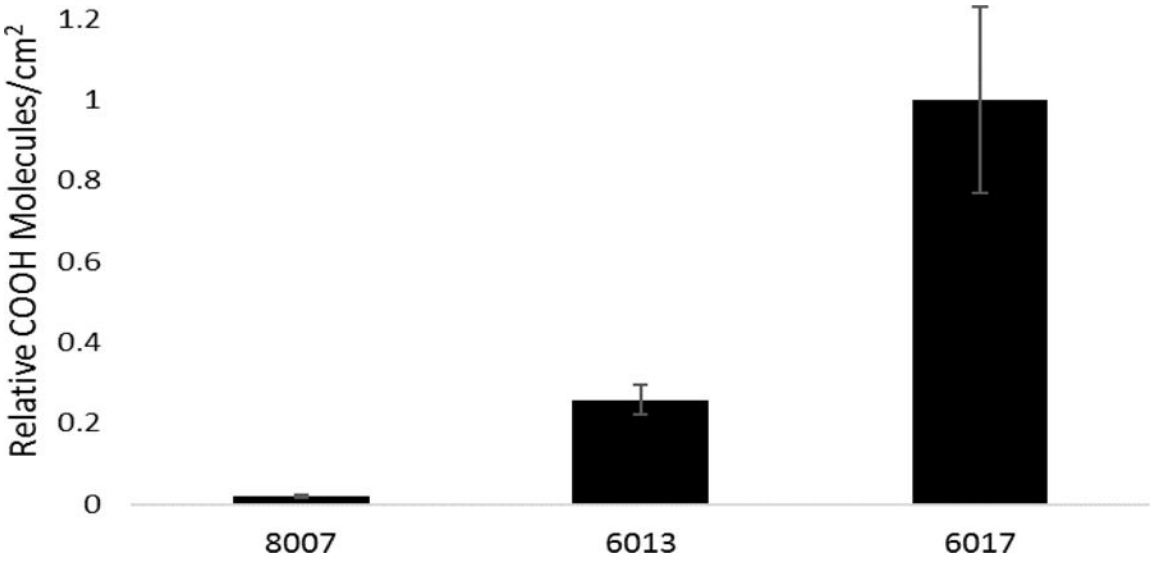

Figure 7.

TBO assay to probe surface -COOH molecule numbers for various UV/O_3 (21.85 mW/cm^2) activated COC substrates. Results show the relative –COOH molecules/cm^2, normalized with respect to COC 6017, which showed the highest –COOH functional group density. As the norbornene increased, the relative amount of –COOH molecules increased as well. Error bars represent ±std of the relative –COOH molecules/cm^2 (n=3).

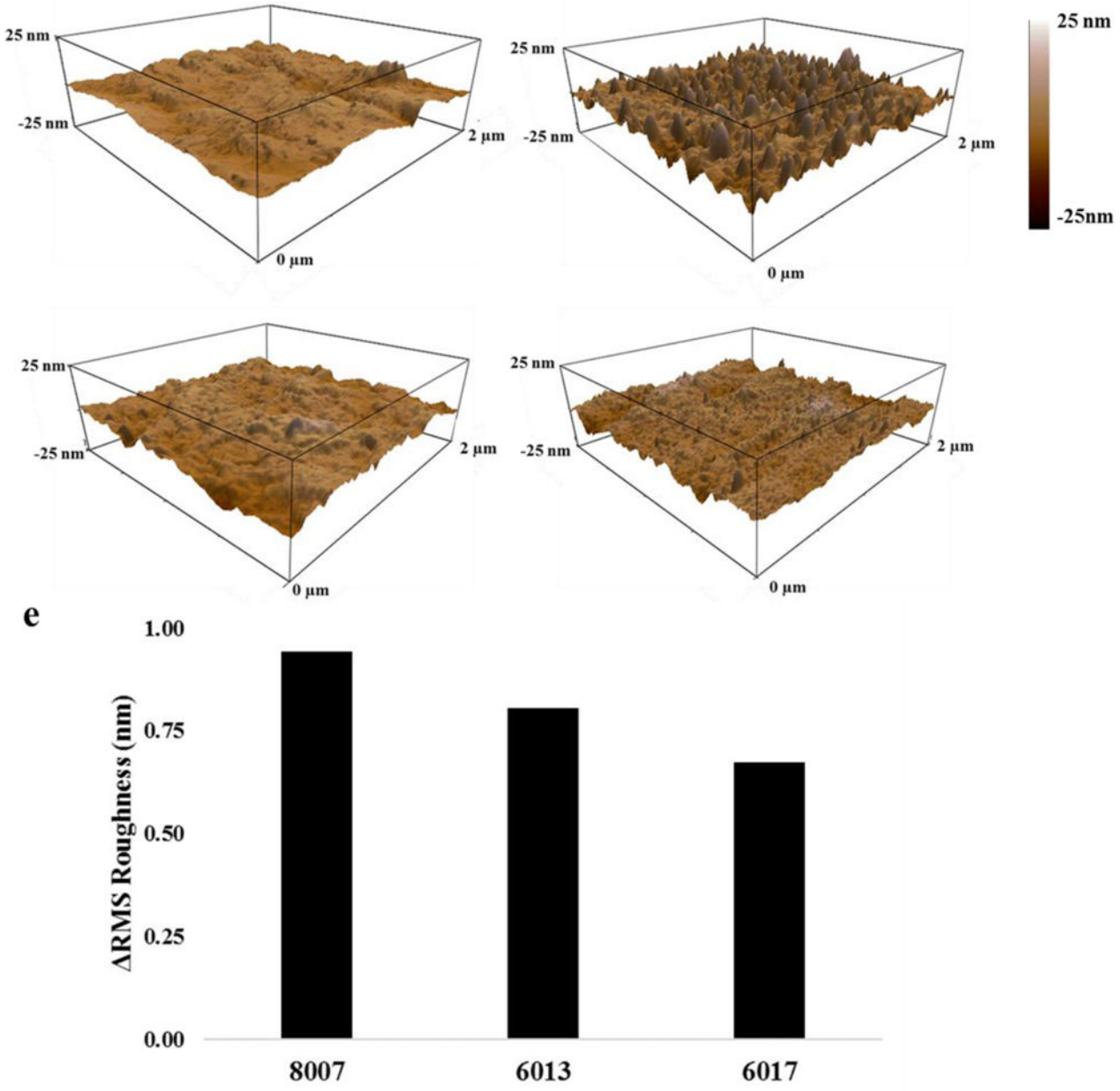

Figure 8.

AFM images of COC 8007 a) native and b) 50 W 30 s O_2 plasma -treated compared to COC 6017 c) native and d) 50 W 30 s O_2 plasma -treated substrates. An increase in surface roughness upon activation for both substrates was observed with greater RMS roughness noted for COC 8007. e) The change in the RMS roughness versus the COC grade confirming that an increase in the norbornene mol % showed a decrease in the RMS roughness. Raw data can be found in Table S2.

Table 1

Common Polymers and their physiochemical properties

Material	T_g (°C)	CTE (α) (ppm $°C^{-1}$)	Refractive Index	Young's Modulus (Gpa)	Near UV Transmissivity	Visible Transmissivity
PDMS	−125	67.3	1.40	0.36–0.87 $\times 10^{-3}$	Excellent	Excellent
PC	145–148	60–70	1.584	2.0–2.4	Poor	Excellent
PMMA	100–122	70–150	1.492	1.8–3.1	Good	Excellent
COC	70–170	60–80	1.53	2.6–3.2	Excellent	Excellent

Table 2

Table showing the glass transition temperature (Tg) as a function of the % norbornene content for commercially available TOPAS COC as depicted in panel 2.

TOPAS Name	T_g (°C)	Norbornene mol %
8007	75	35
6013	130	50
6017	170	60

TOPAS COC